# Impedance and Corrosion Resistance Characteristics of Reanodized Anodic Alumina Film on AA 5052

## Naveen Verma[*], Krishan C Singh, Jitender Jindal, Anuj Mittal

*Department of Chemistry, Maharshi Dayanand University, Rohtak-124001, Haryana, India*

## ABSTRACT

*Complex anodic alumina films were preapered by the reanodization of porous anodic oxide films on aluminium alloy (AA) 5052. The AA 5052 samples were anodized first in $H_2SO_4$ for 30 min at 15 V. The reanodization was performed in 0.1 M ammonium pentaborate solution at 15 V for 5 and 10 min. Electrochemical impedance spectroscopy was employed to characterize these complex films. Polarization studies show that the corrosion rate decreases significantly by reanodization and it is further decreases with an increase in reanodization time. Reanodization is found a good method to increase corrosion resistance properties of porous anodic oxide film. Morphologically, no significant difference was observed between simple and complex film as shown in Field Emission Scanning Electron Microscope (FESEM) images. The electrochemical impedance data was fitted with equivalent circuit containing a Constant Phase Element (CPE) and fitted parameters were calculated.*

**Keywords:** AA 5052, Ammonium pentaborate, FESEM, EIS

## INTRODUCTION

Anodic oxide films were formed by the process of anodic oxidation of metal in suitable electrolyte. Aluminum and its alloys are widely used in industry, so extensively investigated to know the electrochemical behavior in various electrolytes [1-3]. Anodic oxide film with varying properties over a wide range can be obtain just by choosing the anodization conditions, especially the electrolyte composition and applied voltage or current [3-5]. Mainly barrier and porous type anodic oxide films were formed during anodization on aluminum. The formation of barrier or porous type film depends on the electrolyte composition, temperature, applied voltage or current density or other anodization conditions [6]. The porous alumina films have received a new technological application in the field of nanotechnology, like fabrication of nanomaterials such as nanotubes, nanowires, nanodots etc, [7-11]. Other than these applications the anodic oxide film increases the corrosion resistance properties of metals by providing a barrier oxide film [12,13]. Barrier films were formed during anodization in an electrolyte which does not dissolve the film [14]. The passive thin film blocks the dissolution of the metal in corrosive environment. The barrier-type anodic oxide layer on aluminium and its alloys are also used as a dielectric layer in aluminium electrolytic capacitors. The electrical properties of capacitors depend upon the dielectric characteristics and dimensions of anodic oxide film in relation to the electrochemical oxidation process for film formation [15-17]. The anodic oxide film on aluminum and its alloys obtained in sulfuric acid solution commonly consists of two layers; a thick porous outer layer in contact to the electrolyte separated from the metal by a thin non-porous compact uniform layer called the barrier layer [18,19]. These films are widely used as protective, decorative, electro insulating and hard coatings [20,21]. Porous $Al_2O_3$ was found one of the most favorable ceramics sensing materials [22]. The small pore radius in porous alumina makes it sensitive to very low vapor pressure [23]. Besides the barrier and porous films, the complex films were also formed when a porous film is reanodized [14,24,25]. The complex films have improved electrical and corrosion resistance properties [24,26]. Reanodization of the porous $\alpha$-$Al_2O_3$ in certain acid solutions at low voltage was found to be an effective humidity sensor at various temperatures [27]. The knowledge of bulk and surface characteristics of anodic oxide film has great importance to utilize porous and complex films (Reanodized in neutral electrolyte). In this work, electrochemical Impedance Spectroscopy (EIS) and potentiodynamic polarization were used to study the influences of reanodization on the electrochemical behaviour of anodized AA 5052. AA 5052 is commonly used for the manufacture of kitchen cabinets, small boats, home freezers, air craft tube. The motivation behind this study was to investigate the possibility of improving the surface and corrosion resistance properties of anodic oxide films by reanodization in ammonium pentaborate solution.

## EXPERIMENTAL

Samples of AA 5052 with the exposed area of 1 cm$^2$ were used as working electrode. AA 5052 has following composition 0.35% Cr, 0.15% Cu, 2.2% Mg, 0.1% Mn, 0.4% silicon + iron and balance Al. First of all, the specimen samples were mechanically polished with silicon carbide paper for the smooth surface appearance followed by chemical etching with NaOH (100 g/l). Anodization was performed in a simple

electrochemical cell with a magnetic stirrer under the constant temperature of 30°C. A Platinum mesh was used as the cathode. The samples were placed at the centre of the platinum mesh. In the present investigation, Al 5052 samples were anodized in 0.3 M $H_2SO_4$ at 15 V for 30 min (Sample A). Then these anodized samples were reanodized in 0.1 M ammonium pentaborate solution at 15 V for 5 min (Sample B) and 10 min (Sample C). The oxide films were characterized by microscopy, impedance spectroscopy and polarization measurements. The morphology was studied by FESEM (Zeiss Ultra 55, Oxford instruments) in high vacuum. The impedance and polarization measurements were done by potentiostat (Auto lab) having three electrode set up in which Ag/AgCl is used as a reference electrode. All the electrochemical measurements were done in 1 M KCl solution. The frequency range applied for impedance measurements is $10^{-1}$ Hz to $10^5$ Hz.

## RESULTS AND DISCUSSION

The anodic porous layer on the AA 5052 sample consists of double layer; one is called as barrier layer intact to the metal surface and another is porous layer which is present above this barrier layer. The complex films were formed by reanodization of porous oxide film samples in near neutral electrolytes (Ammonium pentaborate) which partially filled the pores. The thickness of the barrier layer increases after reanodization [24].

To evaluate the electrochemical characteristics and corrosion resistance properties of anodized and reanodized samples, the Nyquist and Bode plots from electrochemical EIS were shown in Figure 1. In Figure 1(a), the shape and diameter of the capacitive loop curves presented the corrosion resistance properties of anodic oxide film [28]. Corrosion resistance properties are directly proportional to the diameter of loop i.e. Bigger the diameter of the loop, better are the corrosion resistance properties [29,30]. The capacitive loops for reanodized complex films are much bigger than the simple anodized sample (Figure 1a). Furthermore, the loop size increases with an increase in reanodization time from 5 to 10 min. This indicate that, reanodization of porous oxide film contribute towards increase in corrosion resistance properties due to increase in thickness of barrier film.
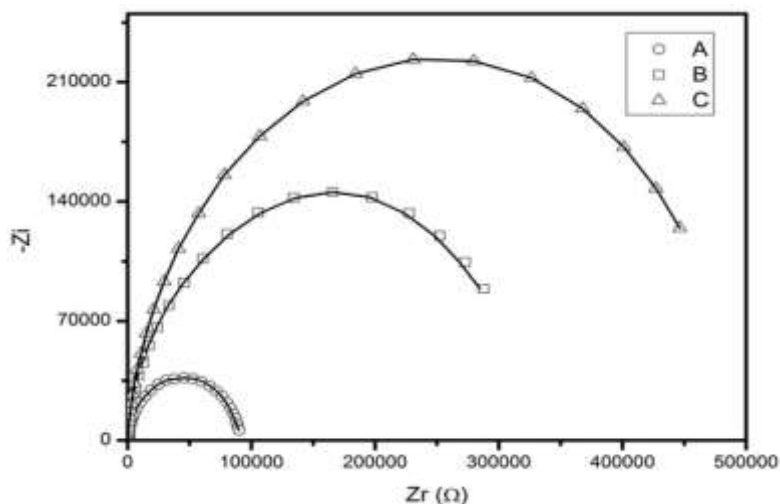


**Figure 1a: Nyquist plots of (A) porous type film; (B) reanodized for 5 min; (C) reanodized for 10 min, lines represents the fitted curve**

The increase in impedance exhibits an improvement of anodic oxide film on reanodization. The result of Bode Plots in Figure 1(b) and (c) exhibit the similar trend as in Nyquist plots showing reliability of experimental results. The maximum experimental phase (Bode Plots) angle near to 90° indicates the nature of electric double layer formation and higher stability of the oxide film (Figure 1c).
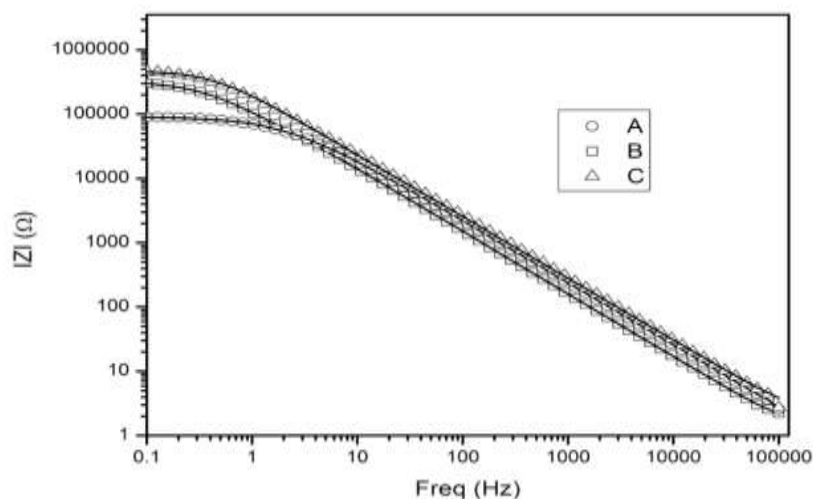


**Figure 1b: Bode plots modulus of (A) porous type film; (B) reanodized for 5 min; C) reanodized for 10 min, lines represents the fitted curve**
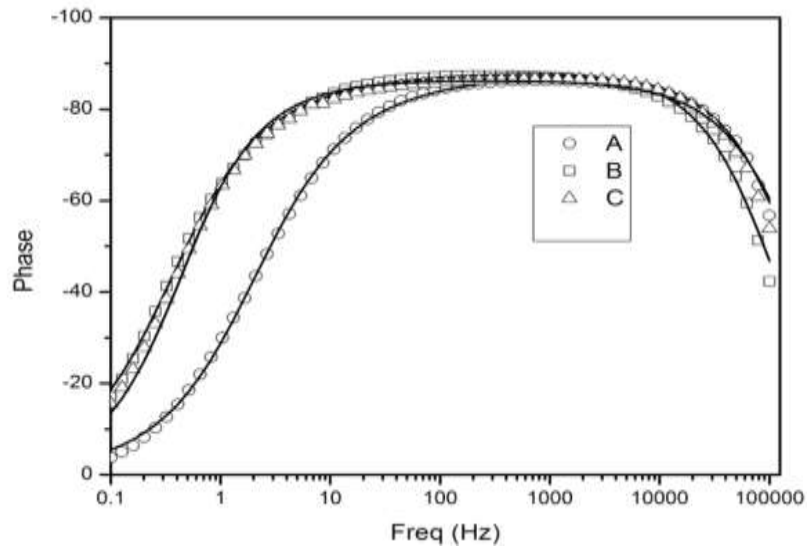
**Figure 1c: Bode plots phase of A) porous type film; B) reanodized for 5 min; C) reanodized for 10 min, lines represents the fitted curve**

The phase angle is found near to 90° in wide frequency range, in reanodized samples (B and C), as compare to simple porous alumina sample (A) indicating improvement anodic oxide film on reanodization [31]. Slight shifts of phase-angle minima towards the low-frequency region indicate an increase in the porous layer resistance [32]. At frequencies higher than 1 Hz bode magnitude displayed linear slopes indicating a typical capacitive behavior [12]. The experimental impedance data were fitted with Z view software and the good agreement was observed between the experimental results and simulated curve proving that the proposed model is appropriate. We interpreted the spectra by using an equivalent circuit having a resistance R, a modeling element with frequency distribution behavior called as constant phase element (CPE) and $R_{el}$, resistance of the electrolyte (Figure 2). The CPE summarizes the impedance response of a distributed process in an Equation.

$$Z_{CPE} = A-1 \ (i\omega)^{-n}$$

Where, $Z_{CPE}$ is the CPE impedance, A is proportional constant, $\omega$ is the rotation frequency and n has the meaning of a phase shift.
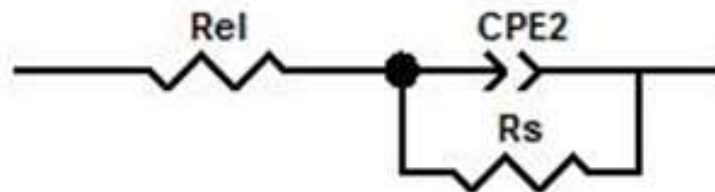


**Figure 2: Equivalent circuit diagram for modeling of impedance data**

The equivalent circuit consisted of a parallel combination of the film resistance R and capacitance CPE, connected in series to the electrolytic resistance $R_{el}$. The CPE are used to account for the irregularities and variations of the properties of various layers. It can be seen from Figure 1, the calculated curve fits well to the experimental data. By simulation with the equivalent circuit, the resistance and capacitance of anodized samples were evaluated given in Table 1. The value of CPE decreases and resistance increases from simple to complex alumina and similar behavior with an increase in reanodization time [23]. This is due to increase in thickness of barrier film by reanodization and the thickness increases with reanodization time.

**Table 1: Evaluated circuit data of the different anodized films (A) porous type film; (B) reanodized for 5 min; (C) reanodized for 10 min**

| Sample | CPE(F) | Rel (ohm) | Rs (ohm) |
|--------|--------|-----------|----------|
| A | $1.3493 \times 10^{-6}$ | 1.46 | $8.5 \times 10^{4}$ |
| B | $1.0103 \times 10^{-6}$ | 1.27 | $3.04 \times 10^{5}$ |
| C | $8.0709 \times 10^{-7}$ | 1.69 | $4.7 \times 10^{5}$ |

**Morphology of the porous films**

FESEM images of sample A and B is shown in Figure 3. The minute pores ranging from 20 to 30 nm were formed and there is no significant difference was observed on surface morphology between the simple porous and reanodized sample for 10 min. Only some degree of smoothness has been observed after reanodization.
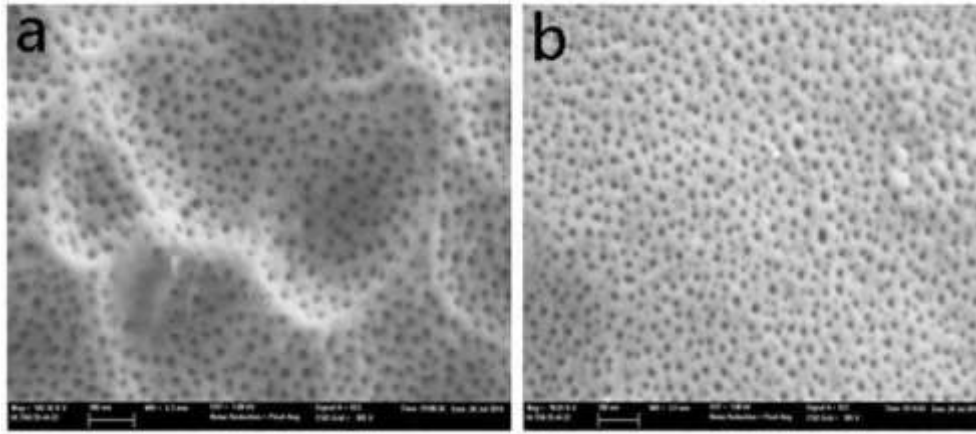
**Figure 3: SEM images of (a) simple porous type film; (b) reanodized for 10 min**

### Corrosion resistance characteristics

The polarization plots of anodized samples were shown in Figure 4 and their corrosion potentials ($E_{corr}$), corrosion current density ($i_{corr}$), Tafel slops ($\beta_a$ and $\beta_c$) and corrosion rate are displayed in Table 2. The measurements are repeated three times. The plot shows that the reanodized samples have more positive $E_{corr}$ and very less corrosion current density as compare to simple anodized samples.

**Table 2: Polarization data of the different anodized films (A) porous type film; (B) reanodized for 5 min; (C) reanodized for 10 min**

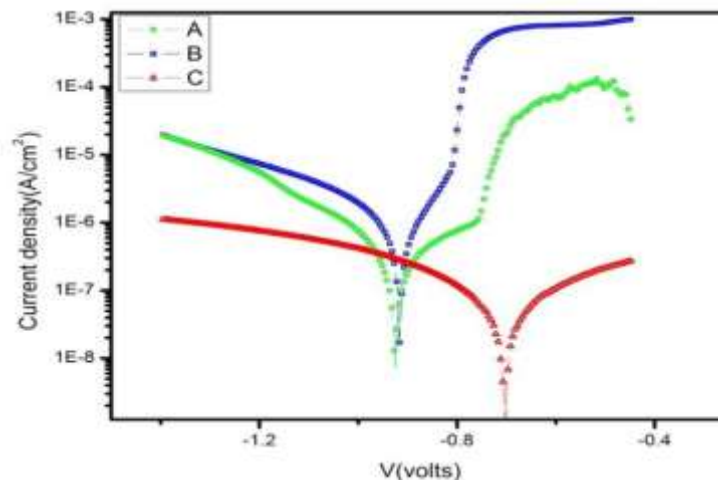| Sample | βa (V/dec) | βc (V/dec) | $E_{corr}$, Obs. (V) | $i_{corr}$ (A/cm²) | Corrosion (mm/year) | Polarization Resistance (Ω) |
|--------|-----------|-----------|----------------------|---------------------|---------------------|------------------------------|
| A | 0.42048 | 0.089994 | -0.91787 | 6.18E-07 | 0.0067403 | 26036 |
| B | 0.26808 | 0.28218 | -0.92685 | 1.75E-07 | 0.0019031 | 171010 |
| C | 0.37502 | 0.43558 | -0.70465 | 3.76E-08 | 0.0004097 | 1.16E+06 |



**Figure 4: Potentiodynamic polarization of (A) porous type film; (B) reanodized for 5 min; (C) reanodized for 10 min**

### CONCLUSIONS

The porous anodic oxide films were fabricated by anodic oxidation of AA 5052 in 0.3 M $H_2SO_4$ solution and reanodized in 0.1 M ammonium pentaborate solution for 5 and 10 min. The impedance spectroscopy was found an appropriate method for characterization of anodic oxide film on aluminum for corrosion resistance characteristics. The corrosion current density was found decreases significantly with reanodization. The increase in anodization time increases the thickness of barrier film by filling of pores which results decrease in the corrosion rate. The increase in corrosion resistance up on reanodization is supported by the impedance data (Nyquist plots) and increase in film resistance calculated by fitting the impedance data with equivalent circuit.

### ACKNOWLEDGEMENT

### REFERENCES

[1] M. Zheng, M. Sakairi, H. Jha, *Corros. Sci.*, **2012**, 55, 332.
[2] S. Feliu, M.J. Bartolome, J.A. Gonzalez, V. Lopez, S. Feliu, *Appl. Surf. Sci.*, **2008**, 254, 2755.

[3] S.J. Ma, P. Luo, H. Zhou, C. Fu, Y. Kuang, *Trans. Nonferrous Met. Soc. China.*, **2008**, 18, 825.

[4] H. Habazaki, K. Shimizu, P. Skeldon, G.E. Thompson, G.C. Wood, *Thin Solid Films.*, **1997**, 300, 131.

[5] S. Gudic, J. Radosevic, D. K. Lisica, M. Kliski, *Electrochim. Acta.*, **2001**, 46, 2515.

[6] W. Lee, S.J. Park, *Chem. Rev.*, **2014**, 114, 7487.

[7] E. Lefeuvre, K.H. Kim, Z.B. He, J.L. Maurice, M. Chatelet, D. Pribat, C.S. Cojocaru, *Thin Solid Films.*, **2011**, 519, 4603.

[8] Y. Wang, S. Shimada, Y. Yamamoto, N. Miyaura, *Mater. Re.s Bull*., **2008**, 43, 251.

[9] R. E. Sabzi, K. Kant, D. Losic, *Electrochim. Acta.*, **2010**, 55, 1829.

[10] S. Ye, Y. Hou, R. Zhu, S. Gu, J. Wang, Z. Zhang, S. Shi, J. Du, *J. Mater. Sci. Technol.*, **2011**, 27, 165.

[11] S.H. Jeong, H.Y. Hwang, S.K. Hwang, K.H. Lee, *Carbon.*, **2004**, 42, 2073.

[12] J. Wang, C. Li, S. Zheng, C.Y. Yin, Y.H. Wang, *Trans. Nonferrous Met. Soc. China.*, **2014**, 24, 3023.

[13] Q. Li, Y. Tang, Y. Zuo, *Mater. Chem. Phys.*, **2010**, 120, 676.

[14] S. Wernick, R. Pinner, Corrosion Protection and Control Using Nanomaterials, Teddington, Middlesex, England, **1987**.

[15] A. Mozalev, M. Sakairi, H. Takahashi, H. Habazaki, J. Hubalek, *Thin Solid Films.*, **2014**, 550, 486.

[16] M. Monta, Y. Matsuda, *J. Power Sources.*, **1996**, 60, 179.

[17] H.J. Oh, G.S. Park, J.G. Kim, Y. Jeong, C.S. Chi, *Mater. Chem. Phys.*, **2003**, 82, 331.

[18] K. Nielsch, J. Choi, K. Schwirn, R.B. Wehrspohn, U. Gosele, *Nanoletters.*, **2002**, 2, 677.

[19] J.P. Dasquet, D. Caillard, E. Conforto, J.P. Bonino, R. Bes, *Thin Solid Films.*, **2000**, 371, 183.

[20] D. Gilroy, P.J. Eddowes, I.M. Dalrymple, I. Azkarate, V. Madina, F. Seco, A.D. Barrio, J. Parkes, M. Byrne, R. Byrne, E.M. Almeida, A. Maia, D. Pereira, F.L. Bentes, *Metal Finishing.*, **1996**, 94, 28.

[21] E.W. Brooman, *Metal Finishing.*, **2002**, 100, 104.

[22] H. Farahani, R. Wagiran, M.N. Hamidon, *Sensors.*, **2014**, 14, 7881.

[23] L.H. Mai, P.T. Hoa, N.T. Binh, N.T. Ha, D. Khac, *Sens. Actuators B. Chem.*, **2000**, 66, 63.

[24] A. Girginov, A. Popova, I. Kanazirski, A. Zahariev, *Thin Solid Films.*, **2006**, 515, 1548.

[25] A. Dekker, A. Middelhoek, *J. Electrochem. Soc.*, **1970**, 117, 440.

[26] M. Machkova, E. Klein, A. Girginov, S. Ikonopisov, *Surf. Technol.*, **1984**, 22, 21.

[27] Z. Chen, M.C. Jin, In Appl. Soc 27th Annual Conf. IEEE Industry, Houston TX, **1992**, 1668.

[28] D.C. Garrido, D.M.O. Toledo, J. Hernández, J.G. Rodriguez, J. Uruchurtu, *J. Solid State Electrochem.*, **2009**, 13, 1715.

[29] F. Zhu, J. Wang, S. Li, J. Zhang, *Appl. Surf. Sci.*, **2012**, 258, 8985.

[30] G. Song, A.L. Bowles, D.H. John, *Mat. Sci. Eng. A.*, **2004**, 366, 74.

[31] Z. Liu, X. Liu, U. Donatus, G.E. Thompson, P. Skeldon, *Int. J. Electrochem. Sci.*, **2014**, 9, 3[558.

[32] M. Franco, S. Anoop, R.U. Rani, A.K. Sharma, *ISRN Corrosion.*, **2012**, 12.